Theory of the asymmetric ripple phase in achiral lipid membranes

2011 EPL 95 48004

(http://iopscience.iop.org/0295-5075/95/4/48004)

A Letters Journal Exploring the Frontiers of Physics

August 2011

EPL, **95** (2011) 48004
doi: 10.1209/0295-5075/95/48004

www.epljournal.org

Theory of the asymmetric ripple phase in achiral lipid membranes

Md. Arif Kamal[1], Antara Pal[1], V. A. Raghunathan[1(a)] and Madan Rao[1,2]

[1] *Raman Research Institute - C V Raman Avenue, Bangalore 560 080, India*
[2] *National Centre for Biological Sciences (TIFR), GKVK Campus - Bangalore 560 065, India*

received 1 April 2011; accepted in final form 1 July 2011
published online 1 August 2011

PACS 87.16.D- – Membranes, bilayers, and vesicles
PACS 61.30.Dk – Continuum models and theories of liquid crystal structure

Abstract – We present a phenomenological theory of phase transitions in achiral lipid membranes in terms of two coupled order parameters —a scalar order parameter describing *lipid chain melting*, and a vector order parameter describing the *tilt of the hydrocarbon chains* below the chain-melting transition. Existing theoretical models fail to account for all the observed features of the phase diagram, in particular the detailed microstructure of the *asymmetric ripple phase* lying between the fluid and the tilted gel phase. In contrast, our two-component theory reproduces all the salient structural features of the ripple phase, providing a unified description of the phase diagram and microstructure.

Phospholipids self-assemble in water to form a rich variety of spatially modulated phases [1]. The simplest of these is the one-dimensionally modulated fluid lamellar phase (L_α) consisting of periodic stacks of lipid bilayer membranes separated by water, where the hydrocarbon chains are floppy with liquid-like in-plane order. Changing the temperature or water content induces a sequence of symmetry-breaking transitions characterized by unique microstructures.

On reducing the temperature below the chain-melting (main) transition (T_m), the L_α phase of phosphatidylcholines (PCs) transforms to a gel phase ($L_{\beta'}$), characterized by fully stretched *all-trans* chains which are tilted with respect to the bilayer normal [2–4]. In addition, an *asymmetric ripple phase* ($P_{\beta'}$) is found to occur in between the L_α and $L_{\beta'}$ phases in many PCs at high water content [1,2,5].

Extensive studies using a variety of experimental techniques [1,6–18], reveal that the $P_{\beta'}$ phase is characterized by a periodic saw-tooth height modulation of the bilayers having an amplitude of ∼1 nm and a wavelength of ∼15 nm, and a bilayer thickness that is different in the two arms of the ripple (fig. 1) [9,10]. As a result, the rippled bilayers lack a mirror plane normal to the rippling direction. While in principle, this discrete symmetry breaking can arise from an asymmetry in either *shape* (unequal lengths of the two arms) or *bilayer thickness* (unequal bilayer thickness in the two arms), in practice these asymmetries seem to appear simultaneously.

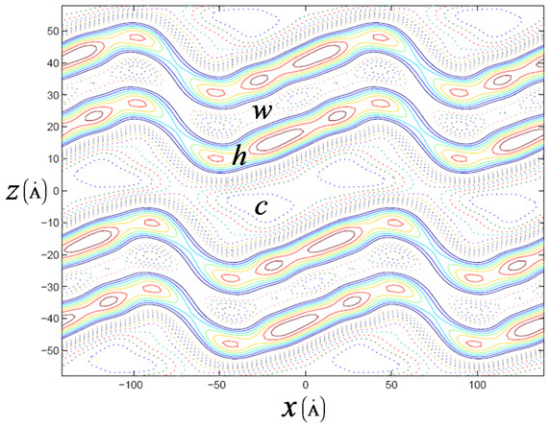

Fig. 1: (Colour on-line) Electron density map of the ripple phase of dimyristoylphosphatidylcholine calculated from X-ray diffraction data [19]. Bands labeled h and c correspond to the headgroup and hydrocarbon chain regions of the bilayer; w denotes the water layer separating the bilayers.

At first it was believed that the origins of the asymmetric ripple lay in the chirality of lipid molecules [20]. However, subsequent experiments using racemic mixtures showed this was not the case [8,15]. More recently, many computer simulations of lipid bilayers have observed that the degree of chain ordering is different in the two arms of the ripple [21–25]. The occurrence of the ripple phase only

(a) E-mail: varaghu@rri.res.in

in those lipids that exhibit a $L_{\beta'}$ phase at lower temperatures [26], and in isolated bilayers [27], suggests an intimate connection between chain tilt and the ability of the bilayers to form ripples.

Several theoretical models have been proposed to describe the sequence of phase transitions in such lipid bilayers and the microstructure of the ripple phase [20,28–38]. None of them accounts for all the observations. We list three key features that should be explained by any theory of the *ripple phase in achiral bilayers* : 1) occurrence of $P_{\beta'}$ phase between L_α and $L_{\beta'}$ phases, separated by two first-order transitions; 2) unequal bilayer thickness in the two arms of the ripple; and 3) unequal lengths of the two arms.

In this paper we present a phenomenological Landau theory to describe the ripple phase in an isolated, achiral lipid bilayer. Our free-energy expression is written in terms of two order parameters: a scalar order parameter ψ and a 2-D vector order parameter $\mathbf{m}$ (fig. 2), and incorporates all terms consistent with the symmetry of the bilayer, to as high an order as is necessary to describe the asymmetric rippled phases (up to 4th order). ψ describes the melting of the bilayer and is the difference in the bilayer thickness [32,33] between the fluid (L_α) and ordered ($P_{\beta'}$ and $L_{\beta'}$) phases. Since the bilayer thickness is determined by the conformations of the hydrocarbon chains, ψ can also be interpreted in terms of differences in chain conformations between the fluid and ordered phases [34]. $\mathbf{m}$ is the projection of the molecular axis $\mathbf{n}$ on the bilayer plane [20]. A third-order parameter h, describing the height of the bilayer, can be integrated out of the expression for the total free-energy density. This model is found to capture all three salient features of the ripple phase listed above.

The total free energy per unit area is taken to be the sum of three terms; the stretching free-energy density f_s, the tilt free-energy density f_t, and the curvature free-energy density f_c. For an isolated lipid bilayer f_s is given by [38],

$$f_s = \frac{1}{2}a_2\psi^2 + \frac{1}{3}a_3\psi^3 + \frac{1}{4}a_4\psi^4 + \frac{1}{2}C\left(\nabla\psi\right)^2 + \frac{1}{2}D\left(\nabla^2\psi\right)^2 + \frac{1}{4}E\left(\nabla\psi\right)^4, \quad (1)$$

where $\psi(x,y) = \frac{\delta(x,y)-\delta_0}{\delta_0}$, $\delta(x,y)$ being the membrane thickness at position (x,y) in the bilayer measured with respect to a flat reference plane, and δ_0 the constant thickness of the membrane in the L_α phase. ψ is taken to be positive for $T < T_m$ due to the stretching of the chains. This is valid in general, even if the chains are tilted below T_m. Explicit temperature dependence is assumed to reside solely in the coefficient of ψ^2 : $a_2 = a_2'(T - T^*)$, T^* being a reference temperature. a_3 is taken to be negative, so that the continuous transition at T^* is preempted by a first-order melting transition at $T_m = T^* + \frac{2a_3^2}{9a_2'a_4}$. The coefficient C can either be positive or negative, but a_4, D and E are always positive to ensure stability. With $C > 0$, the equilibrium phases are always spatially homogeneous; either as L_α or L_β ($L_{\beta'}$). However, with $C < 0$ modulated phases are possible with some characteristic wave vector q_0.

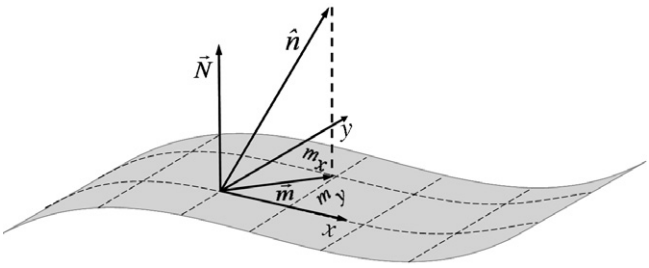

Fig. 2: The unit vector $\mathbf{n}$ represents the orientation of the long axis of the lipid molecules relative to $\mathbf{N}$, the bilayer normal. $\mathbf{m} = \mathbf{n} - (\mathbf{N}\cdot\mathbf{n})\,\mathbf{N}$ is the projection of $\mathbf{n}$ on the bilayer plane.

To motivate how C can be negative, it is convenient to introduce an auxiliary scalar variable ρ. Constructing effective cylinders enclosing the head group and the chain with cross-sectional areas a_h and a_t, respectively, we define $\rho \equiv (a_h - a_t)/(a_h + a_t)$. Consider a bilayer membrane whose thickness ψ increases steadily over a length scale ξ. This variation in thickness produces a strain at the molecular level. This can be accommodated both by a variation in the tilt $\mathbf{m}$, and a variation in the mismatch ρ over this scale. The latter coupling to lowest order is of the form $\nabla\psi\cdot\nabla\rho$. This term, consistent with the symmetries of the bilayer, will generically lead to $C < 0$. The $(\nabla\psi)^4$ term is included, since in the context of a one-dimensional model with a scalar order parameter, it has been shown that such a term is necessary to stabilize a modulated phase with a non-zero mean value of the order parameter [39].

The tilt free-energy density can be written as

$$f_t = \frac{1}{2}b_2\left|\mathbf{m}\right|^2 + \frac{1}{4}b_4\left|\mathbf{m}\right|^4 + \tilde{\Gamma}_1\left(\nabla\cdot\mathbf{m}\right)^2 + \Gamma_2\left(\nabla^2\mathbf{m}\right)^2 + \Gamma_3(\nabla\cdot\mathbf{m})^4 + \Gamma_4\psi\left|\mathbf{m}\right|^2 + \Gamma_5\left(\mathbf{m}\cdot\nabla\psi\right)^2 + \Gamma_6\left(\mathbf{m}\times\nabla\psi\right)^2 + \Gamma_7\left(\nabla^2\psi\right)\left(\nabla\cdot\mathbf{m}\right)^2 + \Gamma_8(\nabla\psi)^2(\nabla\cdot\mathbf{m})^2. \quad (2)$$

The first four terms in eq. (2) are the usual terms in the expansion of the free energy in terms of a vector order parameter [20]. The $(\nabla\cdot\mathbf{m})^4$ term is included to be consistent with the $(\nabla\psi)^4$ term introduced in f_s. The next term represents the coupling between ψ and $\mathbf{m}$, which is responsible for the appearance of tilted phases in this model, as b_2 is taken to be positive. If $\Gamma_4 > 0$, the stable phase below T_m is L_β with $|\mathbf{m}| = 0$. On the other hand, tilted phases can form if $\Gamma_4 < 0$. Note that the coefficients Γ_4 and C are closely related, since a positive mismatch ρ ($a_h > a_t$) automatically gives rise to a tilt in the gel phase, consistent with the experimental observation that the ripple phase forms in systems that have a tilted gel phase.

The subsequent terms reflect the natural coupling between thickness modulation and tilt, taking into account the anisotropy of the tilted bilayer. The higher-order coupling terms between modulations in thickness and tilt are kept merely for consistency and are not crucial for obtaining the optimal phases.

The curvature energy density of the bilayer can be written as [20,35],

$$f_c = \frac{1}{2}\kappa \left(\nabla^2 h\right)^2 - \gamma \left(\nabla^2 h\right)(\nabla \cdot \mathbf{m}), \tag{3}$$

where $h(x,y)$ is the height of the bilayer relative to a flat reference plane, κ is the bending rigidity of the membrane, and γ couples the mean curvature to splay in $\mathbf{m}$.

The equilibrium height profile of the bilayer $h(x,y)$ is related to the tilt $\mathbf{m}$ via the Euler-Lagrange equation,

$$\nabla^2 h = \frac{\gamma}{\kappa}(\nabla \cdot \mathbf{m}). \tag{4}$$

Eliminating h from the free-energy density f leads to the effective energy density $f_{\rm eff}$ with a reduced splay elastic constant $\Gamma_1 = \tilde{\Gamma}_1 - \gamma^2/(2\kappa)$.

To determine the mean-field phase diagram we choose the following variational ansatz for ψ and $\mathbf{m}$:

$$\begin{aligned} \psi &= \psi_0 + \psi_1 \sin(qx), \\ m_x &= m_{0x} + m_{1x}\cos(qx) + m_{2x}\sin(qx) \\ &\quad + m_{3x}\cos(2qx) + m_{4x}\sin(2qx), \\ m_y &= m_{0y}, \end{aligned} \tag{5}$$

with the amplitudes $\{\psi_i, m_i\}$ as variational parameters. We retain Fourier components of m_x to second order to account for the ripple asymmetry; the experimentally observed asymmetric ripple profile is obtained if $m_{3x} \neq 0$. In principle, we could have done a numerical variational calculation with all Fourier components. However, our simplified ansatz is sufficient to recover all the qualitative features of the experimentally observed asymmetric ripple phase. We however do not capture the exact phase boundaries and sharper features of the profiles.

We have not included 2D modulations of the membrane [40] in our ansatz given in eq. (5), since earlier studies [20,35,37] based on a similar free-energy density for the tilt and curvature alone show that the presence of a mean tilt suppresses two dimensional height modulations. The additional ψ-dependent terms in the free-energy density do not alter this conclusion, hence we confine our attention to one-dimensionally modulated ripples. Note that spatial modulations in m_y are neglected as we do not keep terms proportional to $(\nabla \times \mathbf{m})$ in eq. (2) for reasons discussed below.

The phase diagram in the C-T plane obtained from numerical minimization of the effective free-energy density averaged over one spatial period, $\langle f_{\rm eff}\rangle = (q/2\pi)\int_0^{2\pi/q} f_{\rm eff}\mathrm{d}x$, is given in fig. 3. It is calculated for

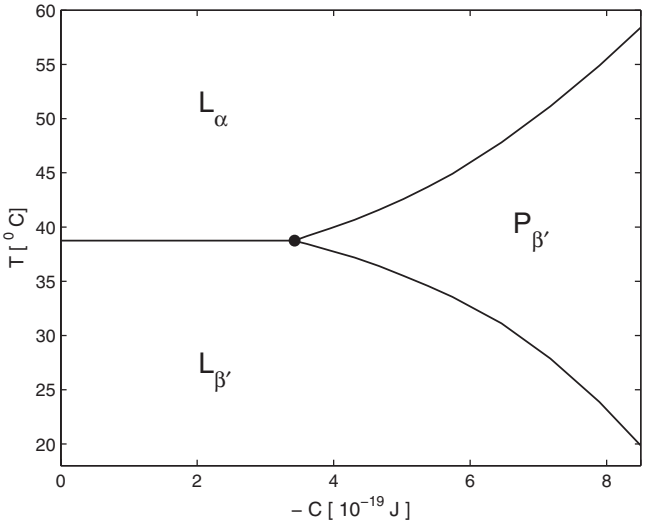

Fig. 3: Phase diagram in the C-T plane calculated from the model. $a_2' = 159.42\,k_B$, $T^* = 260\,\mathrm{K}$. Values of the other coefficients in units of $k_B T^*$ are: $a_3 = -306.5$, $a_4 = 613.15$, $b_2 = 0.2$, $b_4 = 200$, $D = 557.41$, $E = 600$, $\Gamma_1 = 0.010$, $\Gamma_2 = 1.80$, $\Gamma_3 = 500$, $\Gamma_4 = -3$, $\Gamma_5 = -20$, $\Gamma_6 = -20$, $\Gamma_7 = -50$, $\Gamma_8 = -25$. Both the main transition ($L_\alpha \to L_{\beta'}$; $L_\alpha \to P_{\beta'}$) and pre-transition ($P_{\beta'} \to L_{\beta'}$) are first order.

a choice of parameter values, which reproduce closely the main- and pre-transition temperatures of dipalmitoylphosphatidylcholine at $C = -4.84 \times 10^{-19}$J. The values of T^*, a_2, a_3, a_4 and D are similar to those used in refs. [33,38]. As can be seen from fig. 3, there are three distinct regions in the phase diagram corresponding to three different phases: $L_\alpha(\psi_0 = \psi_1 = m_{0x} = m_{0y} = m_{1x} = m_{2x} = m_{3x} = m_{4x} = 0)$, $L_{\beta'}(\psi_0 \neq 0,\ m_{0x} \neq 0,\ m_{0y} \neq 0;\ \psi_1 = m_{1x} = m_{2x} = m_{3x} = m_{4x} = 0)$, and $P_{\beta'}(\psi_0 \neq 0,\ \psi_1 \neq 0,\ m_{0x} \neq 0,\ m_{2x} \neq 0,\ m_{3x} \neq 0;\ m_{1x} = m_{4x} = m_{0y} = 0)$.

The $P_{\beta'}$ phase obtained from the model has a saw-tooth–like height profile and has the same symmetry as the experimentally observed structure. The first-order transition lines which separate these three phases meet at a Lifshitz point located at $C_{Lp} = -3.43 \times 10^{-19}$J and $T = 38.75\,^\circ$C. For $C > C_{Lp}$, the first-order $L_{\beta'} \to L_\alpha$ transition line is parallel to the C axis and occurs at $T_m = 38.75\,^\circ$C. But for $C < C_{Lp}$, the intermediate $P_{\beta'}$ phase is found, separated from the other two phases by first-order transition lines. Further, the region occupied by the $P_{\beta'}$ phase expands at the expense of the other two as C becomes more negative.

Typical spatial variation of the order parameters in the ripple phase is shown in fig. 4. The height profile is asymmetric and resembles very closely those seen in experiments (fig. 1) [9,10,18]. ψ_1 is almost $\pi/2$ out of phase with h, so that it is positive (negative) along the longer (shorter) arm of the ripple, resulting in different bilayer thicknesses in the two arms, again in agreement with experimental observations (fig. 1) [9,10]. Figure 5 shows a schematic of the structure of the bilayer inferred from these results. It is clear that the model presented

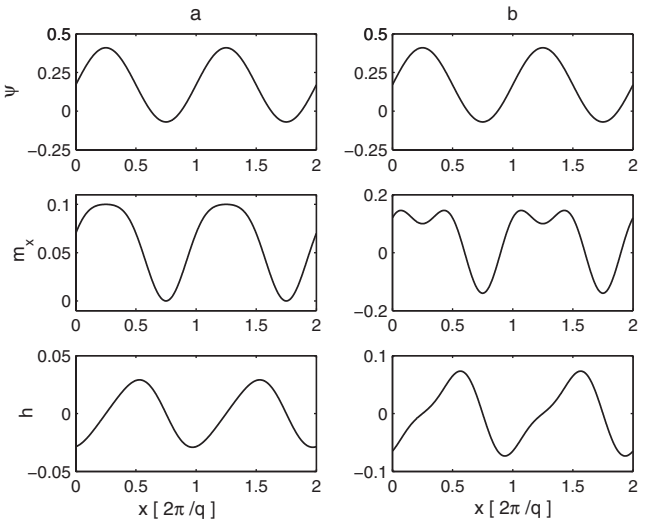

Fig. 4: Spatial variation of the different order parameters in the $P_{\beta'}$ phase at $T = 310.50\,\mathrm{K}$ and $C = -5.02 \times 10^{-19}\,\mathrm{J}$. (a) for $\Gamma_5 = \Gamma_6 = \Gamma_7 = \Gamma_8 = 0$, and all other parameter values as in fig. 3; (b) for all parameter values as in fig. 3.

here accounts for all the salient features of the ripple phase listed in the introduction.

The present model predicts the chain tilt to be high in the thicker arm and negligible in the thinner one. There are in principle at least two chain conformations consistent with this thinner arm of the bilayer —one is by having disordered chains, the other by chain interdigitation. Since in our model, the high-temperature phase was identified as L_α, it is natural to populate the thinner arm with disordered chains. We therefore propose that in the asymmetric ripple, the thicker arm is made up of tilted gel-like domains and the thinner one is fluid-like with negligible chain tilt. This conclusion is partially supported by spectroscopy and diffusion experiments, which indicate a significant fraction of disordered chains in the ripple phase [41,42]. However, it must be acknowledged that there is no direct experimental data on the spatial distribution of the disordered chains within the rippled bilayer. Electron density maps such as the one shown in fig. 1 do not provide any direct information about chain ordering. In contrast, recent computer simulation studies of the ripple phase using a variety of model lipids at different levels of coarse-graining [21,23,25], find an asymmetric ripple structure consistent with the height and thickness modulations seen in the electron density maps, with the thicker arm consisting of gel-like domains, and the thinner one made up of ordered and interdigitated chains. The crossover region between these two contains a large fraction of disordered chains. In the gel-like domains chains are tilted with respect to the local layer normal, whereas chain tilt vanishes in the thinner arm due to interdigitation. Thus the height, thickness and tilt modulations found in these simulations are consistent with the predictions of the present model, although the thinner arm consists of interdigitated chains instead disordered

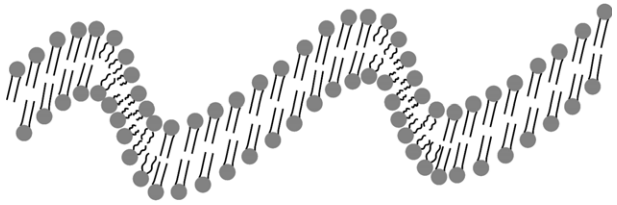

Fig. 5: Schematic of the bilayer profile obtained from the model. Note that the bilayer thickness is different in the two arms of the saw-tooth–like ripples.

chains as proposed here. Symmetric ripples consisting of alternating gel-like and fluid-like domains have also been found in some simulations [22]. These ripples are characterized by only a thickness modulation and no height modulation. Stacks of such bilayers will result in a centered rectangular lattice and do not seem to have been observed in any pure lipid-water system.

The $\Gamma_4 \psi\, m^2$ term in the free-energy expression which produces the chain tilt below the main transition for $\Gamma_4 < 0$, also leads to a bilayer ripple even in the absence of any of the higher-order coupling terms. This ripple has $m_{0x} \neq 0$, and is weakly asymmetric, with m_{3x} typically an order of magnitude smaller than m_{2x} (fig. 4(a)). Thus the present model spontaneously picks out a non-zero value of the mean tilt along the ripple direction q, even in the absence of any explicit in-plane anisotropy of the bending rigidity ($\Gamma_5 = \Gamma_6 = 0$). This is in contrast to the model presented in refs. [20] and [35], where the mean tilt occurs in a direction normal to q, resulting in a symmetric ripple in the case of achiral bilayers; the bending rigidity has to be explicitly taken to be lower along the tilt direction in order to obtain a non-zero mean tilt along q and to stabilize asymmetric ripple within this model [37]. The asymmetry of the ripple is enhanced by the higher-order coupling terms with negative coefficients (fig. 4(b)).

It would seem that our free-energy functional contains a large number of parameters, which we need to fine tune to obtain the asymmetric ripple phase. We would like to emphasize that asymmetric ripples are a fairly generic and robust feature of our model *whenever* $\Gamma_4 < 0$. The other Γ_i's only make the shape anisotropy in the height profile more pronounced when they are negative, and are not crucial for the existence of the asymmetric ripple phase. Further, X-ray diffraction experiments identify the asymmetric ripple phase on the basis of its oblique unit cell. Such a unit cell can arise either from a strongly asymmetric height profile or from a weakly asymmetric height profile as long as the thickness is different in the two arms of the ripple [37]. This feature is exactly what is captured within our theory (figs. 4(a) and 4(b)).

Another type of ripple phase with $m_{2x} = m_{3x} = 0$, but with $m_{1x} \neq 0$ and $m_{4x} \neq 0$ is obtained for relatively high positive values of Γ_7. Here ψ_1 and h are almost in phase, so that the bilayer thickness is modulated within each arm of the ripple. Such a structure does not seem to have been observed in any experiments. It might be possible to tune

this parameter by a suitable choice of an impurity which would prefer to smoothen variations in ψ; in such cases we predict the existence of this new ripple phase.

We have only included terms proportional to $(\nabla \cdot \mathbf{m})$ in the expression for f_t. In general there will also be terms proportional to $(\nabla \times \mathbf{m})$, which lead to a ripple structure with a non-zero winding number in the model presented in refs. [20] and [35]. However, such a structure can be expected to be energetically costly in an achiral bilayer, since it is not consistent with parallel close-packing of the chains demanded by van der Waals interaction.

A straightforward extension of this model would be to use a better description of the chain-melting transition, instead of the reduced bilayer thickness ψ employed here. Possible order parameters include components of the in-plane density wave, as considered in the theory of weak crystallization [43], and those of herringbone order, used to describe positional ordering in monolayers [44]. However, such an attempt would be useful only if the details of chain ordering in this phase, presently unknown, can be experimentally established.

* * *

We thank Yashodhan Hatwalne for many valuable discussions and Kheya Sengupta for the electron density map of the ripple phase.

REFERENCES

[1] Tardieu A., Luzzati V. and Reman F. C., *J. Mol. Biol.*, **75** (1973) 711.
[2] Smith G. B., Sirota E. B., Safinya C. R. and Clark N. A., *Phys. Rev. Lett.*, **60** (1988) 813; Smith G. B., Sirota E. B., Safinya C. R., Plano R. J. and Clark N. A., *J. Chem. Phys.*, **92** (1990) 4519.
[3] Sun W.-J., Sutter R. M., Knewtson M. A., Worthington C. R., Tristam-Nagle S., Zhang R. and Nagle J. F., *Phys. Rev. E*, **49** (1994) 4665.
[4] MacIntosh T. J., *Biophys. J.*, **294** (1980) 237.
[5] Janiak M. J., Small D. M. and Shipley G. G., *J. Mol. Biol.*, **254** (1979) 6068.
[6] Wack D. C. and Webb W. W., *Phys. Rev. Lett.*, **61** (1988) 1210.
[7] Hentschel M. P. and Rustichelli F., *Phys. Rev. Lett.*, **66** (1991) 903.
[8] Katsaras J. and Raghunathan V. A., *Phys. Rev. Lett.*, **74** (1995) 2022.
[9] Sun W.-J., Tristam-Nagle S., Sutter R. M. and Nagle J. F., *Proc. Natl. Acad. Sci. U.S.A.*, **93** (1996) 7008.
[10] Sengupta K., Raghunathan V. A. and Katsaras J., *Phys. Rev. E*, **68** (2003) 031710.
[11] Mortensen K., Pfeiffer W., Sackmann E. and Knoll W., *Biochim. Biophys. Acta*, **945** (1988) 221.
[12] Luna E. J. and McConnell H. M., *Biochim. Biophys. Acta*, **470** (1977) 303.
[13] Krbecek R., Gebhardt C., Gruler H. and Sackmann E., *Biochim. Biophys. Acta*, **554** (1979) 1.
[14] Hicks A., Dinda M. and Singer M. A., *Biochim. Biophys. Acta*, **903** (1987) 177.
[15] Zasadzinski J. A. N., *Biochim. Biophys. Acta*, **946** (1988) 235.
[16] Meyer H. W., *Biochim. Biophys. Acta*, **1302** (1996) 138.
[17] Zasadzinski J. A. N., Scheir J., Gurley J., Elings V. and Hansma P. K., *Science*, **239** (1988) 1013.
[18] Woodward J. T. and Zasadzinski J. A., *Biophys. J.*, **72** (1997) 964.
[19] Sengupta Kheya, PhD Thesis, Jawaharlal Nehru University (2000).
[20] Lubensky T. C. and Mackintosh F. C., *Phys. Rev. Lett.*, **71** (1993) 1565.
[21] de Vries A. H., Yefimov S., Mark A. E. and Marrink S. J., *Proc. Natl. Acad. Sci. U.S.A.*, **102** (2005) 5392.
[22] Kranenburg M. and Smit B., *J. Phys. Chem. B*, **109** (2005) 6553.
[23] Lenz O. and Schmid F., *Phys. Rev. Lett.*, **98** (2007) 058104.
[24] Sun X. and Gezelter J. D., *J. Phys. B*, **112** (2008) 1968.
[25] Jamróz D., Kepczynski M. and Nowakowska M., *Langmuir*, **26** (2010) 15076.
[26] Watts A., Harlos K., Maschke W. and Marsh D., *Biochim. Biophys. Acta*, **510** (1978) 63.
[27] Mason P. C., Gaulin B. D., Epand R. M., Wignall G. D. and Lin J. S., *Phys. Rev. E*, **59** (1999) 3361.
[28] Doniach S., *J. Chem. Phys.*, **70** (1979) 4587.
[29] Falkovitz M. S., Seul M., Frisch H. L. and McConnell H. M., *Proc. Natl. Acad. Sci. U.S.A.*, **79** (1982) 3918.
[30] Marder M., Frisch H. L., Langer J. S. and McConnell H. M., *Proc. Natl. Acad. Sci. U.S.A.*, **81** (1984) 6559.
[31] Carlson J. M. and Sethna J. P., *Phys. Rev. A*, **36** (1987) 3359.
[32] Goldstein R. E. and Leibler S., *Phys. Rev. Lett.*, **61** (1988) 2213.
[33] Goldstein R. E. and Leibler S., *Phys. Rev. A*, **40** (1989) 1025.
[34] Honda K. and Kimura H., *J. Phys. Soc. Jpn.*, **60** (1991) 1212.
[35] Chen C.-M., Lubensky T. C. and Mackintosh F. C., *Phys. Rev. E*, **51** (1995) 504.
[36] Seifert U., Shillcock J. and Nelson P., *Phys. Rev. Lett.*, **77** (1996) 5237.
[37] Sengupta K., Raghunathan V. A. and Hatwalne Y., *Phys. Rev. Lett.*, **87** (2001) 055705.
[38] Shimokawa N., Komura S. and Andelman D., *Eur. Phys. J. E*, **26** (2008) 197.
[39] Jacobs A. E., Grein C. and Marsiglio F., *Phys. Rev. B*, **29** (1984) 4179.
[40] Yang L. and Fukuto M., *Phys. Rev. E*, **72** (2005) 010901.
[41] Wittebort R. J., Schmidt C. F. and Griffin R. G., *Biochemistry*, **20** (1981) 4223.
[42] Schneider M. B., Chan W. K. and Webb W. W., *Biophys. J.*, **43** (1983) 157.
[43] Kats E. I., Lebedev V. V. and Muratov A. R., *Phys. Rep.*, **228** (1993) 1.
[44] Kaganer V. M., Möwald H. and Dutta P., *Rev. Mod. Phys.*, **71** (1999) 779.